Received: 8 October 2021 | Revised: 9 December 2021 | Accepted: 9 December 2021

DOI: 10.1111/epi.17154

Epilepsia®

FULL-LENGTH ORIGINAL RESEARCH

Mutations associated with epileptic encephalopathy modify EAAT2 anion channel function

Peter Kovermann | **Yulia Kolobkova** | **Arne Franzen** | **Christoph Fahlke**

Molekular- und Zellphysiologie (IBI-1) Forschungszentrum Jülich, Institute of Biological Information Processing, Jülich, Germany

Correspondence
Peter Kovermann and Christoph Fahlke, Molekular- und Zellphysiologie (IBI-1), Forschungszentrum Jülich, Institute of Biological Information Processing, Jülich 52428, Germany.
Emails: p.kovermann@fz-juelich.de; c.fahlke@fz-juelich.de

Present address
Yulia Kolobkova, Medical School Hamburg, University of Applied Sciences, Hamburg, 20457, Germany

Funding information
German Ministry of Education and Research, Grant/Award Number: 01GM19007

Abstract

Objective: Mutations in the gene solute carrier family member 1A2 (*SLC1A2)* encoding the excitatory amino acid transporter 2 (EAAT2) are associated with severe forms of epileptic encephalopathy. EAAT2 is expressed in glial cells and presynaptic nerve terminals and represents the main L-glutamate uptake carrier in the mammalian brain. It does not only function as a secondary active glutamate transporter, but also as an anion channel. How naturally occurring mutations affect these two transport functions of EAAT2 and how such alterations cause epilepsy is insufficiently understood.

Methods: Here we studied the functional consequences of three disease-associated mutations, which predict amino acid exchanges p.Gly82Arg (G82R), p.Leu85Pro (L85P), and p.Pro289Arg (P289R), by heterologous expression in mammalian cells, biochemistry, confocal imaging, and whole-cell patch-clamp recordings of EAAT2 L-glutamate transport and anion current.

Results: G82R and L85P exchange amino acid residues contribute to the formation of the EAAT anion pore. They enlarge the pore diameter sufficiently to permit the passage of L-glutamate and thus function as L-glutamate efflux pathways. The mutation P289R decreases L-glutamate uptake, but increases anion currents despite a lower membrane expression.

Significance: L-glutamate permeability of the EAAT anion pore is an unexpected functional consequence of naturally occurring single amino acid substitutions. L-glutamate efflux through mutant EAAT2 anion channels will cause glutamate excitotoxicity and neuronal hyperexcitability in affected patients. Antagonists that selectively suppress the EAAT anion channel function could serve as therapeutic agents in the future.

KEYWORDS
epilepsy, gain-of-function, glutamate transporter, *SLC1A2*

1 | INTRODUCTION

Epileptic encephalopathies (EEs) are severe epilepsy syndromes characterized by early onset, multiple seizure types, and abundant epileptiform electroencephalography (EEG) activity combined with developmental slowing or even regression. Recently, mutations in *SLC1A2* (solute carrier protein member 1A2), the gene encoding the L-glutamate transporter EAAT2 (excitatory amino acid transporter 2), were associated with EE in three different studies.[1–3] All patients exhibited severe developmental and EE, with up to 50 seizures daily under anti-epileptic therapy, profound global delay, and progressive brain atrophy.

EAAT2 is the major L-glutamate transporter of mature astrocytes[4–6] and is also expressed in the presynaptic nerve terminal.[7,8] Its genetic ablation in mice results in lethal spontaneous seizures likely caused by increased extracellular L-glutamate concentrations due to reduced glial L-glutamate uptake.[9] However, EAAT2 is not only a secondary active glutamate transporter but also an anion channel.[10–12] Anion channel dysfunction in the related EAAT1 was recently shown to contribute to the pathophysiology of episodic ataxia 6.[13–16]

We here study the functional consequences of three *SLC1A2* variants associated with EE: c.244G>A (p.Gly82Arg/G82R), c.254T>C (p.Leu85Pro/L85P), and c.866C>G (p.Pro289Arg/P289R) in *h*EAAT2 (NM_004171.3)[1–3] through whole-cell patch clamping after heterologous expression in mammalian cells. All mutations were identified as de novo and pathogenic. G82R has been identified in three unrelated individuals, whereas L85P and P289R were found each in one individual.[1,2] All tested mutations increased anion currents and decreased L-glutamate uptake. Two mutations severely affected the size selectivity of the EAAT2 anion channel, permitting diffusion-mediated L-glutamate release.

Key points

- Epileptic encephalopathy (EE)–associated missense mutations in *SLC1A3* cause amino acid substitutions close to the anion channel pore region of human EAAT2.
- All tested mutations decrease protein expression levels to variable extend and abolish L-glutamate uptake.
- G82R, L85P, and P289R enhance EAAT2 anion channel activity.
- G82R and L85P make the anion channel significantly permeable for L-gluconate and L-glutamate.
- Altered EAAT2 anion channel function is a novel pathological basis of human EE.
- Treatment of EAAT2-associated EEs requires mutant channel inhibition, rather than stimulation of neurotransmitter transporter expression.

2 | MATERIAL AND METHODS

2.1 | Heterologous expression of wild-type and mutant EAATs

The coding region of human EAAT2 (kindly provided by Dr. M. Hediger, Universität Bern, Switzerland) was subcloned into pRcCMV using polymerase chain reaction (PCR)–based strategies. Point mutations and fusions to monomeric yellow fluorescent protein (mYFP), were generated by PCR-based techniques. Transient transfection of HEK293T cells using the $Ca_3(PO_4)_2$ technique was performed as described previously.[17]

2.2 | Knock-down of *LRCC8A* in the HEK293T cells line

Knock-down of human *LRRC8A* (gene encoding for: leucine-rich repeat-containing 8 VRAC subunit A) in the embryonic kidney cell line HEK293T was performed with Crispr/Cas technique (Appendix S1).[18]

2.3 | Electrophysiology

Standard whole-cell patch clamp recordings were performed using an Axopatch 200B amplifier (Molecular Devices) as described previously described.[19,20] Cells were clamped to 0 mV or −70 mV for at least 5 s between test sweeps. Junction potentials were corrected a priori. Standard bath solution contained (in mM): 140 NaCl, 4 KCl, 2 $CaCl_2$, 1 $MgCl_2$, 10 HEPES, ±0.5 Na-glutamate, pH 7.4, and standard pipette solutions (in mM): 115 KCl or 115 NaCl, 2 $MgCl_2$, 5 EGTA, 10 HEPES, pH 7.4. In all experiments with K^+ in the pipette solution, K^+-outward currents were blocked by 5 mM TEA-Cl in the bath solution. Glutamate transport currents were calculated by subtracting currents before and after addition of 5 mM external L-glutamate after substitution of Cl^- with D-gluconate in internal and external solutions. In the experiments with D-gluconate–based internal and external solutions, the bath solution contained 140 Na-gluconate, 2 Ca-gluconate, 1 Mg-gluconate, 5 TEA-Cl, 10 HEPES/NaOH, pH 7.4, and the intracellular solution 115 K-gluconate, 2 Mg-gluconate, 5 EGTA, 10 HEPES/KOH,

pH 7.4. Because some of the disease-causing mutations increased the D-gluconate permeability, we additionally measured uptake currents as L-glutamate-dependent current increases at the calculated D-gluconate reversal potential (−5.8 mV). D-gluconate and L-glutamate permeabilities were tested either with symmetric D-gluconate–based solutions (140 Na-gluconate/±5 $Na\text{-}glutamate_{ext}$ and 115 $K\text{-}gluconate_{int}$ at pH 7.4) or in bi-ionic measurements (140 NaCl/±0.5 $Na\text{-}glutamate_{ext}$, and 115 $Na\text{-}gluconate_{int}$ or 115 $Na\text{-}glutamate_{int}$ at pH 7.4).

2.4 | Confocal microscopy and biochemical characterization of EAAT fusion proteins

For confocal imaging HEK293T cells expressing mYFP-*h*EAAT2 fusion proteins were plated on poly-L-lysine coated coverslips 24 h after transfection.[16] Images were acquired with a Zeiss LSM780 inverted microscope using a 63×/1.40 NA oil immersion objective in phosphate-buffered saline at room temperature 48 h after transfection. YFP was excited with an argon laser (488 nm), and emission was detected between 543 and 594 nm. Images were analyzed with FIJI image analysis software.[21]

For sodium-dodecyl sulfate polyacrylamide gel electrphoresis (SDS-PAGE) cells were solubilized in 0.4% dodecyl-maltoside for 30 min on ice, transferred 12 h, and then centrifuged for 35 min at 15,781 *g* at 4°C).[16] The concentration of the protein in the supernatant was determined with the bicinchoninic acid assay kit (BCA assay kit, Abcam, ab102536). Expression levels and glycosylation states were estimated as described (Appendix S1).[16,22]

2.5 | Statistical methods

Data were analyzed with a combination of Clampfit (Molecular Devices), SigmaPlot 12.3 (Jandel Scientific), OriginPro 2018G (OriginLab), and Excel (Microsoft Corp.) programs. Current-voltage relationships were constructed by plotting macroscopic current amplitudes determined 150 ms after the voltage step vs the membrane potential. All data are given as means ± 95% confidence intervals (CIs) unless otherwise stated. For statistical analysis of data, one-way or two-way analyses of variance (ANOVAs), or Kruskal-Wallis tests were used with Holm-Sidak post hoc tests with significance levels $^{*}p \leq .05/^{**}p \leq .01/^{***}p \leq .001$, or Dunn's post hoc testing with a threshold of $^{\#}p = .05$. The data that support the findings of this study are openly available in GitHub at https://github.com/peterkovermann/epileptic_encephalopathy_1.

3 | RESULTS

3.1 | EE-associated *SLC1A2* mutations are located in proximity to the EAAT anion channel

EAAT glutamate transport is based on a large-scale rotational-translational movement of the substrate-harboring transport domain,[23–25] and the EAAT anion channel is transiently formed in intermediate positions at the interface between trimerization and transport domains.[11,26,27] Two disease-associated mutations (G82, P289) exchange residues within the trimerization domain that are conserved across mammalian EAATs as well as in mammalian neutral amino acid transporters and bacterial homologs. The remaining one, L85, is only conserved within mammalian SLC1 proteins (Figure 1A). Figure 1B depicts the localization of the three EE-associated mutations, G82R, L85P, and P289R, in an open anion channel EAAT2 model, based on the channel conformation of the prokaryotic sodium-aspartate symporter from *Pyrococcus horikoshii* (Glt_{Ph}), generated.[11] L85 is homologous to F50 in Glt_{Ph}, which projects into the open anion pore in this model,[11] and the substitution of L85 with a negatively charged residue (L85D) was shown to generate partially cation-permeable EAAT2 anion channels.[11] G82 and L85 are both parts of the second transmembrane helix so that R82 likely also projects into the anion conduction pathway. P289 is at the kink of transmembrane helix 5, close to G82 and L85, but not in direct contact with the aqueous conduction pathway. The corresponding mutation P290R has been extensively studied in *h*EAAT1 and shown to cause a pronounced gain-of-function of the EAAT1-associated anion channel.[14,15,28]

3.2 | EE-associated point mutations affect subcellular trafficking of *h*EAAT2

Disease-causing mutations often decrease protein expression/stability or modify the subcellular distribution of affected proteins. We expressed wild-type (WT) and mutant *h*EAAT2 as mYFP fusion proteins transiently in mammalian cells and studied their subcellular localization with confocal imaging as well as biochemical analysis.[14,22,29] Confocal images showed almost exclusive insertion of WT and L85P mYFP-*h*EAAT2 into the surface membrane or in domains in proximity (Figure 1C). In contrast, the expression of G82R and P289R mYFP-*h*EAAT2 resulted in fluorescent staining of intracellular regions. Figure 1D depicts intensities of membrane-localized fluorescences of individual transfected cells expressing mYFP-tagged EAAT2 variants normalized to the mean membrane-localized

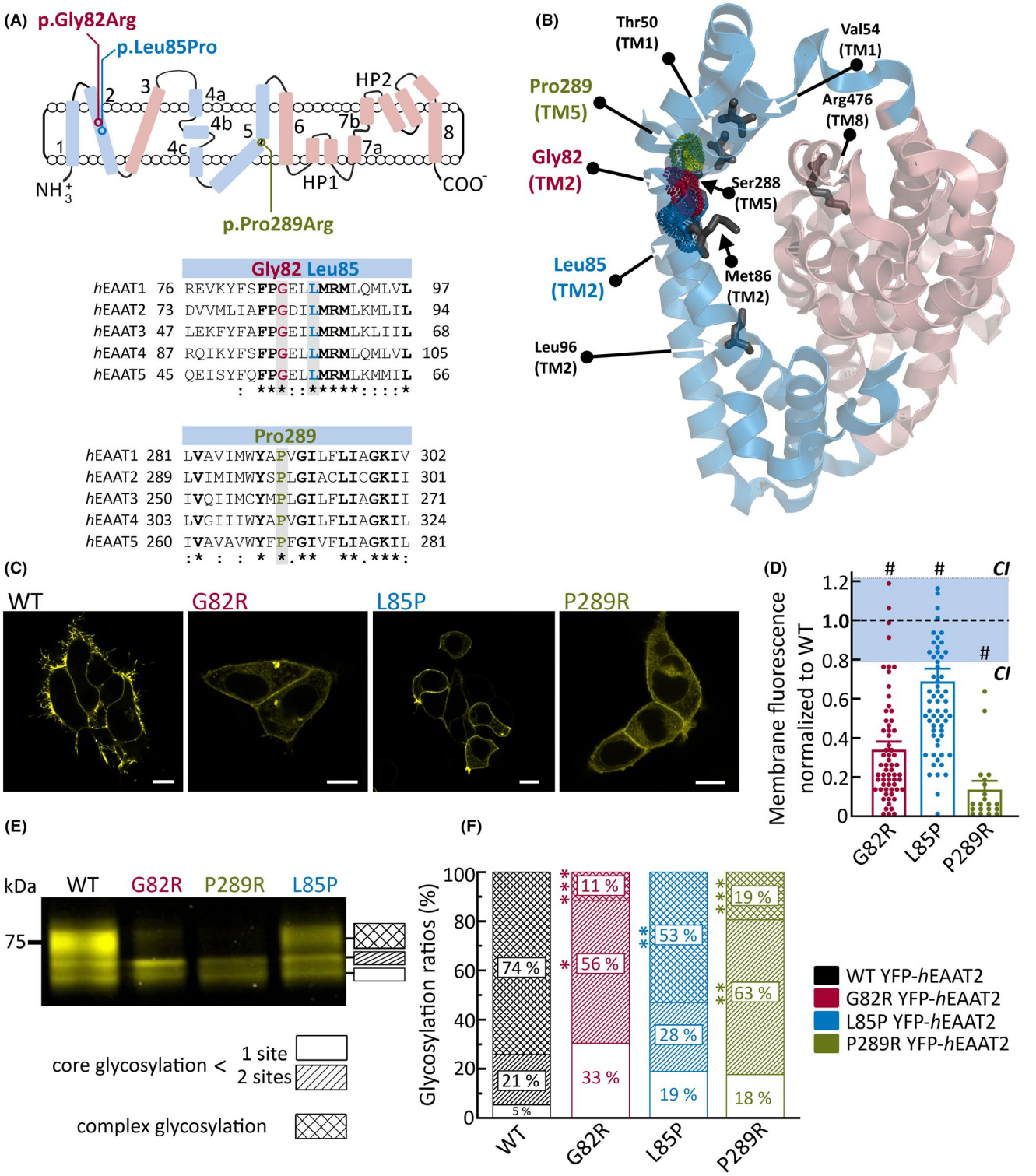

FIGURE 1 Epileptic encephalopathy (EE)–associated missense mutations affect human excitatory amino acid transporter 2 (*h*EAAT2) expression and subcellular trafficking. (A) Positions of EE-associated mutations p.Gly82Arg (NM_004171.3), p.Leu85Pro (NM_004171.3), and p.Pro289Arg (NM_004171.3) in *h*EAAT2 (trimerization/transport domains: blue/magenta). (B) Homology modeling–derived structure of *h*EAAT2 mapped onto the open channel structure from the archaeal aspartate transporter Glt_{Ph} show proximity of affected residues to the anion pore.[12] (C) Confocal images from HEK293T cells expressing WT and mutant *h*EAAT2 fused to yellow fluorescent protein (YFP, scale bars: 10 μm). (D) Relative surface fluorescence of cells expressing mutant *h*EAAT2-YFP. (E) Sodium dodecyl sulfate polyacrylamide gel electrophoresis (SDS-PAGE) analyses from extracted YFP-fusion proteins. (F) Distributions of band intensities from SDS-PAGEs as shown in E. Proportions of glycosylation states in F were analyzed with one-way analysis of variance (ANOVA) for each set of bands separately with WT as control, and Holm-Sidak post hoc testing (*$p \leq .05$, **$p \leq .01$, ***$p \leq .001$). Color code: WT/G82R/L85P/P289R: black/red/blue/green

fluorescences of cells expressing mYFP-tagged WT transporter.

Membrane protein glycosylation is required for exit from the endoplasmic reticulum (ER), and glycosylation levels thus permit quantification of ER exit for WT and mutant *h*EAAT2. In SDS-PAGEs mYFP-*h*EAAT2 appears as a triplicate of fluorescence bands, with molecular sizes between ~60 and 75 kDa. An earlier study demonstrated that the higher molecular-weight band disappears upon deglycosylation with PNGase, but not with EndoH,[30] demonstrating that *h*EAAT2 is complex glycosylated. Whereas the majority of WT and L85P *h*EAAT2 was complex glycosylated, we observed reduced fractions of complex glycosylated protein for G82R and P289R mYFP-*h*EAAT2 (Figure 1E,F). After correcting fluorescence band intensities by transfection efficiencies (Appendix S1 and Figure S1A) we found that the tested EE variants reduced whole protein expression in HEK293T cells to a variable extent (Figure S1B). We conclude that G82R and P289R, but not L85P, impair ER exit and surface membrane expression of *h*EAAT2.

3.3 | EE-associated *SLC1A2* mutations reduce glutamate transport

EAAT2 is a high-capacity glutamate transporter that can generate L-glutamate uptake currents up to 1 nA in transfected mammalian cells.[10,29,31,32] To separate transport currents we substituted Cl^- by D-gluconate, which is impermeant through WT EAAT channels.[32] To measure the unspecific leak component in each experiment, currents were first measured without L-glutamate and then subtracted from current amplitudes obtained after perfusing 5 mM L-glutamate.[10,29] We realized that control currents measured in the absence of L-glutamate were largely increased in cells expressing G82R or L85P *h*EAAT2 (Figure 2A,B). Unlike in cells that express WT EAAT2, these currents do not represent background currents. They do not require L-glutamate and thus are likely caused by D-gluconate permeation through G82R and L85P *h*EAAT2 anion channels. Figure 2C,D depicts representative examples of subtracted current recordings and the voltage dependence of average amplitudes of such current components. WT EAATs transport each L-glutamate together with three Na^+ and one H^+, in exchange with one K^+,[33–35] resulting in pronouncedly voltage-dependent WT *h*EAAT2 transport currents. G82R, L85P, and P289R virtually abolished such currents (−150 mV; −316.4 ± 169.6 pA/−5.6 ± 7.6 pA/−35.4 ± 13.4 pA/−31.1 ± 27 pA, WT/G82R/L85P/P289R, ±CI, n = 10/9/7/7) (Figure 2C,D).

To prevent possible contamination of L-glutamate uptake currents with D-gluconate currents through mutant *h*EAAT2 anion channels, we additionally measured L-glutamate–sensitive currents at the D-gluconate reversal potential, at which any change in channel activity will not modify the current amplitude. Again, we observed drastic reductions in L-glutamate uptake currents for all tested mutant *h*EAAT2 (Figure S2). We conclude that EE-associated *SLC1A2* mutations impair *h*EAAT2 L-glutamate uptake.

3.4 | Pore mutations G82R and L85P modify anion channel function of *h*EAAT2

We next studied the functional consequences of G82R and L85P on *h*EAAT2 anion channels through whole-cell patch clamp in transfected HEK293T cells. In these experiments, solutions were adjusted to salt concentrations that resemble physiological solutions. Cells were internally dialyzed with K^+-based solutions to permit all physiologically occurring transitions in the L-glutamate uptake cycle,[36] and Cl^- was used as the main anion in the internal and the external solution. Experiments were performed under symmetric Cl^- distributions to increase *h*EAAT2 anion currents in the physiological voltage range. Figure 3A shows representative whole-cell current responses to voltage steps between −150 mV and +105 mV from HEK293T cells expressing WT *h*EAAT2 before and after application of 0.5 mM L-glutamate. WT *h*EAAT2 currents were very small in the absence of L-glutamate, and extracellular substrate application (0.5 mM L-glutamate) elicits an inwardly rectifying current component that consists mostly of L-glutamate uptake currents[37] (Figure 3A,B, −150 mV: wo/w L-glutamate: −113.9 ± 34.3/−532.9 ± 145.2 pA, ±CI, n = 12/15). Cells expressing G82R hEAAT2 exhibited currents that change almost linearly with voltage with large current amplitudes without external L-glutamate. Application of L-glutamate did not increase, but rather slightly decreased current amplitudes over the whole voltage range (−150 mV: wo/w L-glutamate: −1742.8 ± 317/−1501.1 ± 582.9 pA, ±CI, n = 11/11) (Figure 3A,B). L85P *h*EAAT2 currents were also much larger than WT currents in L-glutamate-free media; however, L-glutamate augmented currents and generated time- and voltage-dependent changes in amplitude currents (−150 mV: wo/w L-glutamate: −2481.8 ± 803.3/−3408.6 ± 900 pA, ±CI, n = 12/12) (Figure 3A,B). Figure 3B compares current voltage-relationships from whole cell currents for WT, G82R, and L85P *h*EAAT2 in the absence and the presence of external L-glutamate. Because both mutations reduce surface membrane expression levels, this pronounced increase of current amplitudes cannot be due to changes in expression levels. We next correlated

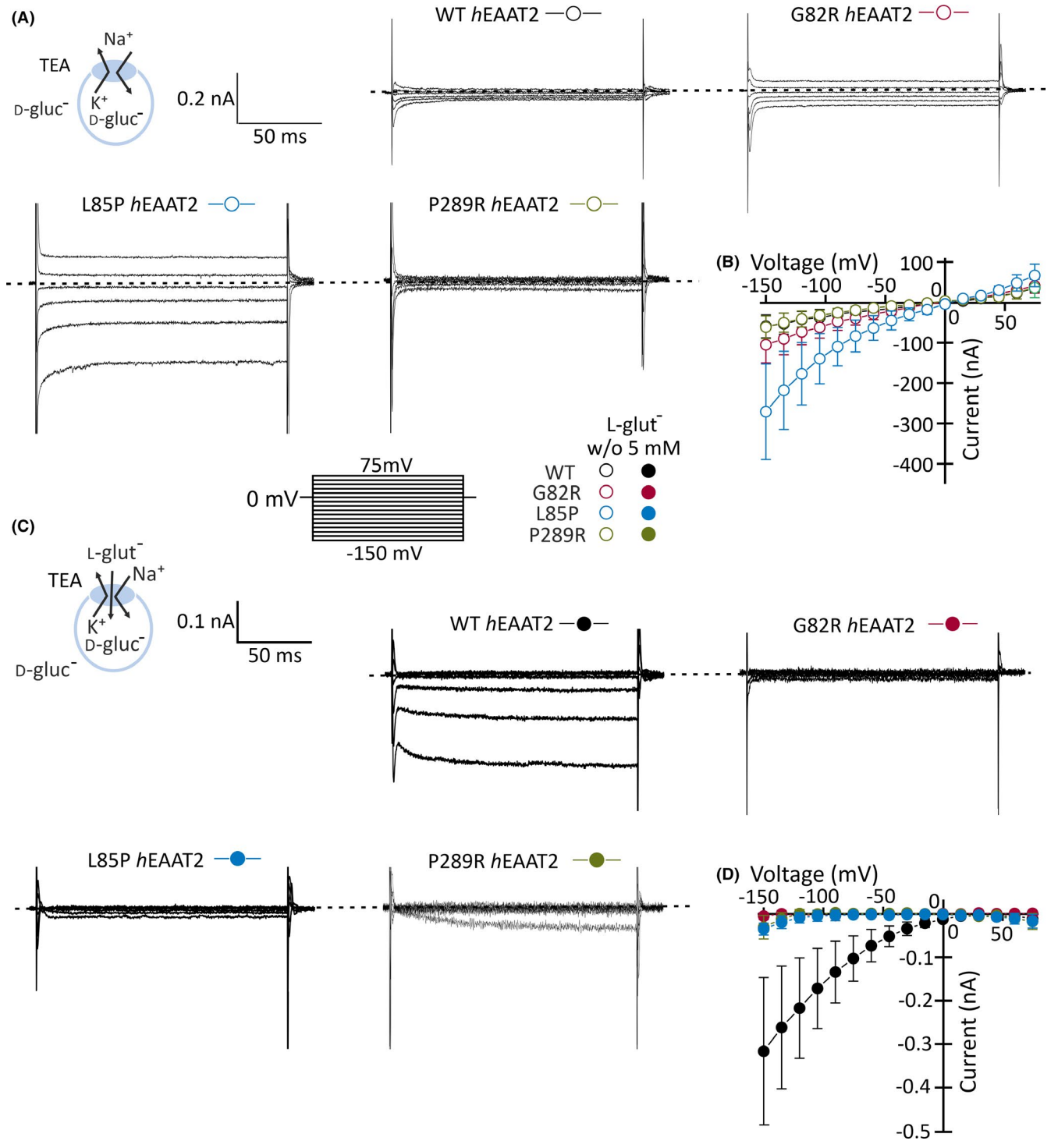

FIGURE 2 Epileptic encephalopathy (EE)–associated mutations impair human excitatory amino acid transporter 2 (*h*EAAT2) -mediated L-glutamate transport. (A) Representative whole-cell current recordings from HEK293T cells expressing wild-type (WT) or the pathogenic variants G82R, L85P, and P289R *h*EAAT2. In these experiments Cl^- is replaced by D-gluconate$^-$, which is impermeant through WT EAAT channels. (B) Mean current-voltage relationships of D-gluconate currents (±CI) for all tested variants. (C) Representative L-glutamate uptake currents from WT and mutant *h*EAAT2 in the presence of 5 mM L-glutamate. (D) Mean uptake current-voltage relationships (±CI) for WT and mutant *h*EAAT2. Color code: WT/G82R/L85P/P289R: black/red/blue/green

single-cell fluorescence amplitudes from mYFP-EAAT2 expressing HEK293T cells with anion channel amplitudes at −150 mV[38,39] (Figure 3C,D and Appendix S1). If the observed anion currents are conducted by mutant *h*EAAT2, a clear correlation between whole-cell current amplitude and the number of expressed fusion proteins,

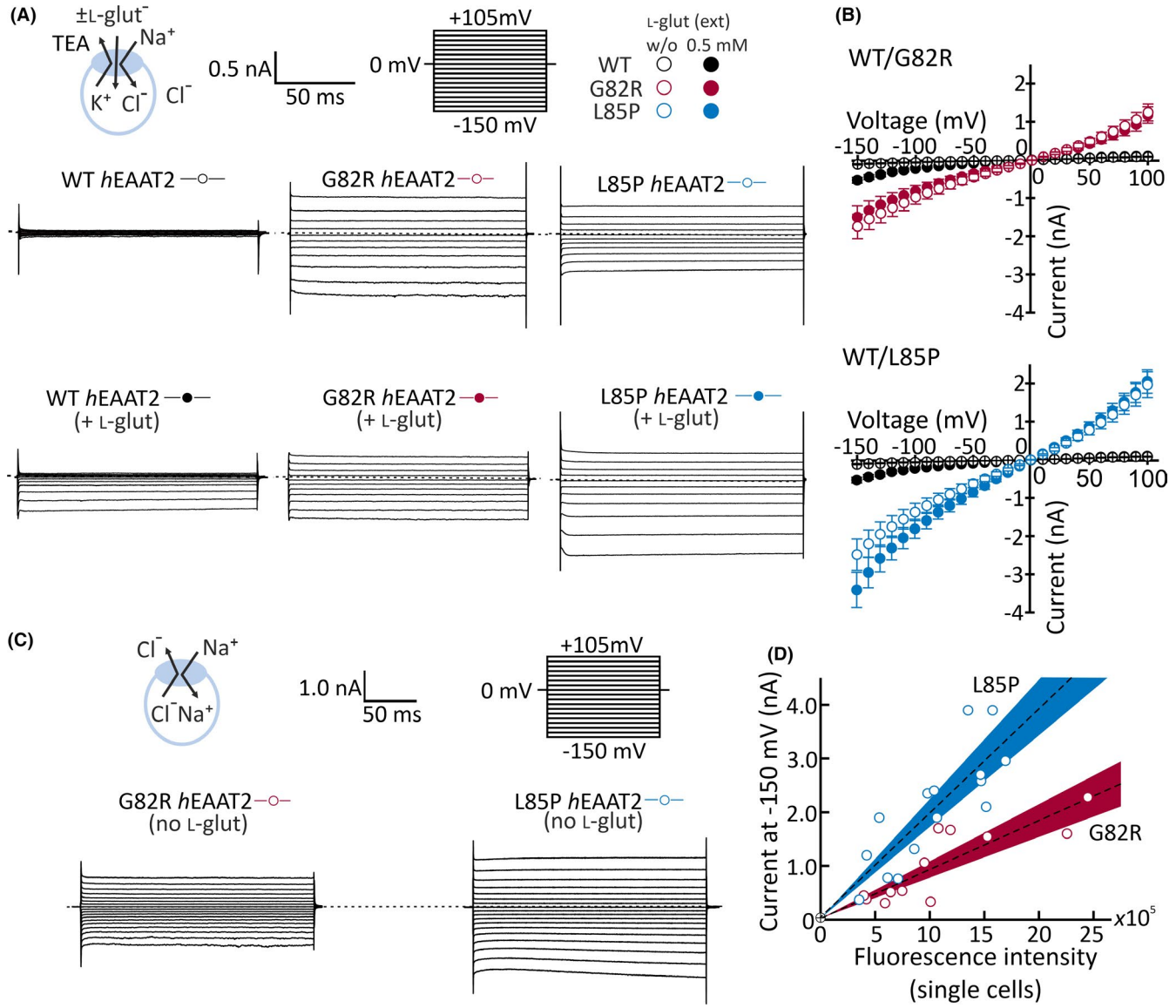

FIGURE 3 Epileptic encephalopathy (EE)–associated missense mutations increase human excitatory amino acid transporter 2 (*h*EAAT2) -associated anion currents. (A) Representative whole-cell current recordings of wild-type (WT) and mutant *h*EAAT2 expressed in HEK293T cells under ionic conditions, which permit transitions between all transporter conformations of *h*EAAT2 (in mM: ±0.5 L-glutamate$^-$/140 $Na^+Cl^-_{ext}$ and 115 $K^+Cl^-_{int}$, see inset), before and after application of 0.5 mM L-glutamate. (B) Mean current-voltage relationships of WT and mutant *h*EAAT2 whole-cell currents in the absence (open symbols) or in the presence (closed symbols) of 0.5 mM L-glutamate. (C) Representative whole-cell current recordings of WT and mutant *h*EAAT2 in the presence of internal and external Na^+Cl^-. (D) Correlation between current amplitudes at −150 mV and yellow fluorescent protein fluorescence amplitudes obtained at the same cell before establishing the whole-cell mode. The lines represent linear regressions ($R^2_{adj,\,G82R} = .91$, $R^2_{adj,\,L85P} = .93$). Data in B are provided as means ± CI. Correlation of whole-cell currents and single cell fluorescence was tested with linear regression and calculation of adjusted R^2 values (R^2_{adj}). The *Y*-axis intercept was manually set to the current amplitude of untransfected cells under the same ionic conditions (22.8 ± 10.4 pA, $n = 5$). Color code: WT/G82R/L85P: black/red/blue

that is, the whole-cell fluorescence, is expected. We found that current amplitudes indeed increase linearly with fluorescence levels ($R^2_{adj,-G82R} = .91$ and $R^2_{adj,-L85P} = .93$) (Figure 3C,D).

Heterologous expression sometimes causes upregulation of endogenous proteins, and volume-activated ion channels (VRACs) seem to be particularly sensitive to such maneuvers.[40] To exclude upregulation of VRACs as a potential source of the large anion currents in cells expressing G82R or L85P *h*EAAT2, we expressed EAAT2 variants in a HEK293T-derived cell, in which a major subunit of the voltage regulated anion channel (VRAC/ LRCC8A, leucine-rich repeat protein 8A)[41] has been knocked out by Crispr-Cas techniques,[18] using the same experimental parameters as in Figure 3A,B. Figure 4 shows representative currents and mean current-voltage relationships

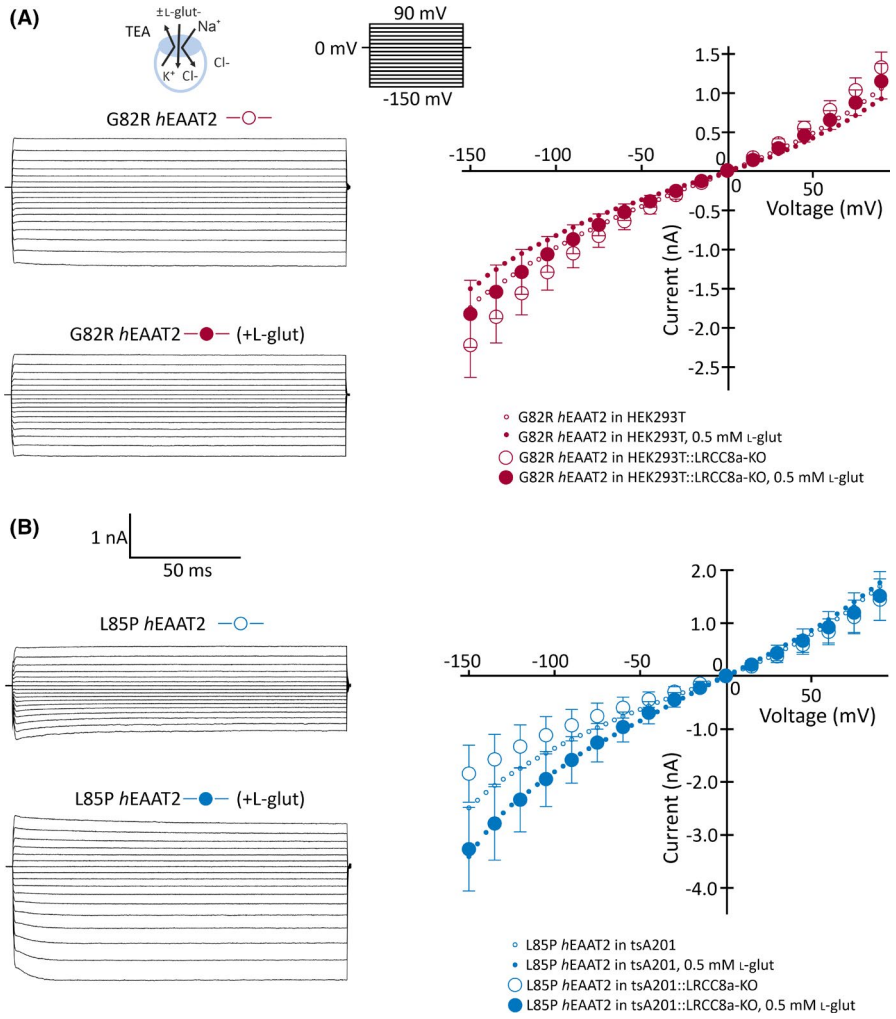

FIGURE 4 G82R and L85P human excitatory amino acid transporter 2 (*h*EAAT2) anion currents in HEK293T cells, in which the gene coding for leucine-rich repeat protein containing 8a (*LRCC8A*) has been genetically removed. (A, B) Representative whole-cell current traces (left column) with corresponding mean current-voltage relationships in the absence (open symbols) and presence (closed symbols) of 0.5 mM L-glutamate (right column, $n = 11/9$, (A) for G82R and L85P ($n = 11/11$, (B) *h*EAAT2 transporters expressed in KO *LRCC8A* HEK293T cells. Mean currents (±CI) of this variants expressed in unmodified HEK293T cell line are provided as small circles (in mM: ±0.5 Na^+-L-glutamate$^-$/140 $Na^+Cl^-_{ext}$, 115 $K^+Cl^-_{int}$). Color code: G82R/L85P: red/blue

from G82R and L85P *h*EAAT2 expressed in KO *LRCC8A* HEK293T cells. We found no differences between anion channel current amplitudes in HEK293T expressing VRAC (dashed lines) or in modified cells (symbols, −150 mV, −2219.9 ± 218.2/−1814.4 ± 274.5 pA, G82R /L85P, ±CI, $n = 11/11$) in the absence of L-glutamate (Figure 4A,B), and perfusion of these cells with external L-glutamate resulted in similar changes in both cell types (−150 mV, 0.5 mM L-glutamate; −1821.8 ± 218.2/3268.5 ± 402.8 pA, G82R/L85P, ±CI, $n = 9/11$) (Figure 4A,B).

3.5 | G82R and L85P render *h*EAAT2 anion channels glutamate permeable

For G82R and L85P *h*EAAT2, we observed currents well above background currents in cells intracellularly dialyzed and external perfused with D-gluconate-based solutions (Figure 2A). These currents demonstrate that D-gluconate can permeate through mutant *h*EAAT2 anion channels. G82R and L85P may thus even allow the passage of L-glutamate through *h*EAAT2 anion channels. We measured reversal potentials of mutant *h*EAAT2 currents in cells internally dialyzed with L-glutamate or D-gluconate-based solutions (Figure 5 and Figure S3) and perfused with physiological Cl^--based external solutions. To prevent possible contaminations with endogenous K^+ channels and to block L-glutamate transport, currents were measured in K^+-free internal and external solutions (in mM, ext: 144 NaCl, 1 $MgCl_2$, 2 $CaCl_2$, 10 HEPES/NaOH; int: 115 Na-gluconate/glutamate, 2 $MgSO_4$, 5 EGTA, 10 HEPES/NaOH, pH 7.4/7.4). Because perfusion with Cl^--based external solutions might result in intracellular Cl^- accumulation, cells were held constantly at −70 mV between voltage steps.

In cells dialyzed with Na-glutamate-based solution (in mM: 115 Na-glutamate, 2 $MgSO_4$, 5 EGTA, 10 HEPES/NaOH), G82R and L85P, but not WT *h*EAAT2 conducted prominent inward currents (Figure 5). Without external L-glutamate, L85P and G82R *h*EAAT2 glutamate currents were significantly larger than WT *h*EAAT2 currents at positive and negative holding potentials (+60 mV:36.2 ±

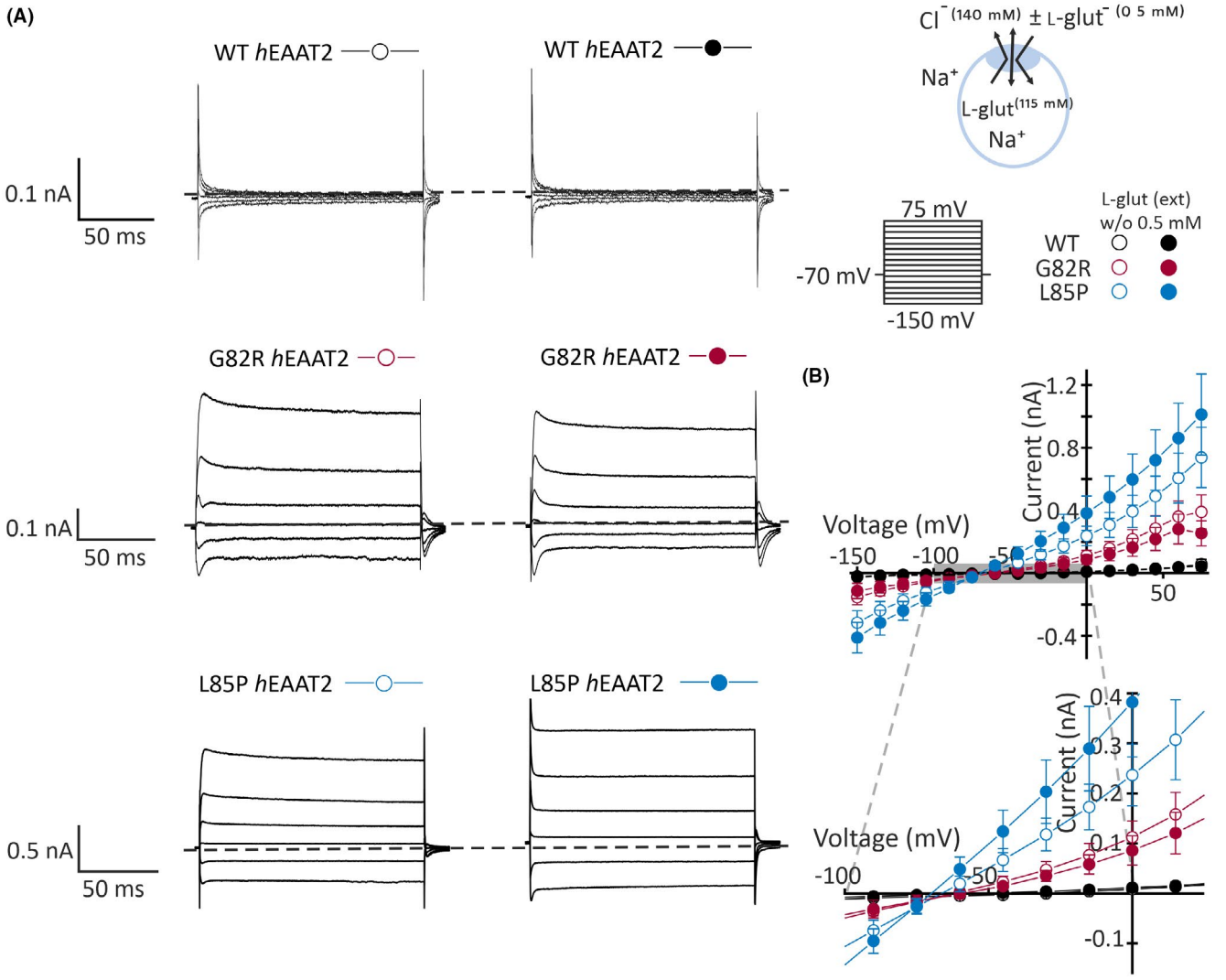

FIGURE 5 Epileptic encephalopathy (EE)–associated variants G82R and L85P render the human excitatory amino acid transporter 2 (*h*EAAT2) anion pore permeable to L-glutamate. (A) Representative G82R and L85P *h*EAAT2 whole-cell currents under ionic conditions, which prevent L-glutamate uptake (in mM: ±0.5 L-glutamate$^-_{ext}$/140 $Na^+Cl^-_{ext}$ and 115 Na^+-L-glutamate$^-_{int}$). (B) Mean current voltage relationships of whole-cell currents from WT, G82R, or L85P *h*EAAT2. The gray-shaded region is magnified as inset. G82R and L85P *h*EAAT2-mediated inward currents correspond to outward permeation of internal L-glutamate. Data in B are provided as means ± CI. Color code: WT/G82R/L85P: black/red/blue

13.8/395.4 ± 117.2/606 ± 158.5 pA; −150 mV: −24.3 ± 5.9 /−162.1 ± 49.8/−316.4 ± 76.3 pA, n = 11/14/11, WT/G82R/L85P). Application of external L-glutamate (0.5 mM) left WT currents nearly unaffected, but increased L85P and decreased G82R inward and outward currents (+60 mV:42.1 ± 10.4/316.6 ± 112.7/861.2 ± 223 pA; −150 mV: −21.5 ± 7.5/−124.3 ± 49.7/−411.6 ± 97.3 pA, n = 9/14/11, WT/G82R/L85P). Reversal potentials from whole-cell currents during perfusion with external NaCl were negative (wo/w: 0.5 mM L-glutamate$_{ext}$, WT: −36.8 ± 9.5/−49.6 ± 16 mV, n = 11/9; G82R: −59.1 ± 7.3/−61.1 ± 6.8 mV, n = 14/14; L85P: −63.2 ± 4/−70 ± 3.4 mV, n = 19/11), indicating lower L-glutamate than Cl^- permeability (Figure S3). We used the Goldman Hodgkin Katz equation to calculate relative permeabilities for G82R $\left(\frac{P_{Glu}}{P_{Cl}} = 0.151 \pm 0.064, N = 14\right.$ (without external L−glutamate) and $\frac{P_{Glu}}{P_{Cl}} = 0.137 \pm 0.051$, $N = 15$ (with external L−glutamate)) and L85P *h*EAAT2 $\left(\frac{P_{Glu}}{P_{Cl}} = 0.117 \pm 0.02, N = 19$ (without external L−glutamate) and $\left.\frac{P_{Glu}}{P_{Cl}} = 0.087 \pm 0.015, N = 11$ (with external L−glutamate)$\right)$ Negligible inward currents demonstrated absent L-glutamate permeability in WT *h*EAAT2 (Figure 5B).

3.6 | P289R modifies opening of *h*EAAT2 anion channel, but not its selectivity

P289R *h*EAAT2 is homologous to P290R *h*EAAT1, which was the first disease-associated *SLC1* mutation linked to neuronal hyperexcitability.[13] The functional consequences of this proline-by-arginine exchange mutation have been studied in *h*EAAT1 in mammalian cells,[13,14] as well as in *h*EAAT3 (P259R) in *Xenopus* oocytes and mammalian cells.[28] In *h*EAAT1 as well as in *h*EAAT3, exchange of proline by arginine increases anion channel open probabilities in the absence as well as in the presence of L-glutamate and causes time-dependent increases of anion currents upon hyperpolarizing voltage steps, a characteristic feature of such mutant transporters that can also be observed in Bergmann glia cells of the transgenic *Slc1a3*$^{P290R/+}$ animals.[15] We did not observe any effects of this mutation on EAAT1/EAAT3 anion channel selectivity or unitary current amplitudes.[14]

Figure 6A depicts representative current recordings from a HEK293T cell expressing P289R *h*EAAT2 under standard conditions before and after L-glutamate application. In the absence of L-glutamate, large mutant anion currents could be observed that were inwardly rectifying, activated upon hyperpolarizing voltage steps, and increased by external L-glutamate application. A comparison of current-voltage relationships from WT and P289R Cl^- currents showed similar current amplitudes at hyperpolarizing potentials (−150 mV: −532.8 ± 74.1/−600.7 ± 174.9 (±CI, n = 12/15, WT/P289R) in the presence of external L-glutamate (−150 mV: −133.9 ± 34.3/−399.1 ± 132.1 pA (n = 12/15) (Figure 6B). However, WT currents predominantly represent electrogenic uptake currents, whereas P289R currents are almost exclusively Cl^- currents, since the mutation abolishes L-glutamate transport currents (Figure 2). P289R *h*EAAT2-mediated D-gluconate currents were indistinguishable from WT (Figure 2), demonstrating unaltered anion channel selectivity of mutant transporters. The increased anion current amplitudes of P289R *h*EAAT2 at lower transporter numbers in the membrane demonstrate gain-of-function of P289R *h*EAAT2-associated anion channels, as observed previously in the episodic ataxia 6-associated P290R mutation in *h*EAAT1.[14]

4 | DISCUSSION

The epileptic encephalopathies (or EEs) are a group of severe and often therapy-resistant early onset epilepsies.[42,43] Severe and frequent seizures, often of distinct generalized epilepsy types, cause cognitive impairment, likely by impairing networks involved in cognitive processing.[42,44] We studied the functional consequences of all *SLC1A2* mutations that have been reported in patients with EE thus far.[1,2] We analyzed how G82R, L85P, and P289R affect glutamate transport, anion channel function, and subcellular localization and protein expression of human EAAT2 in a mammalian cell line as heterologous expression system. These experiments revealed gain-of-anion channel function and reduced L-glutamate transport capability as a major functional alteration for all three mutations. L85P *h*EAAT2 anion currents were larger than current amplitudes recorded

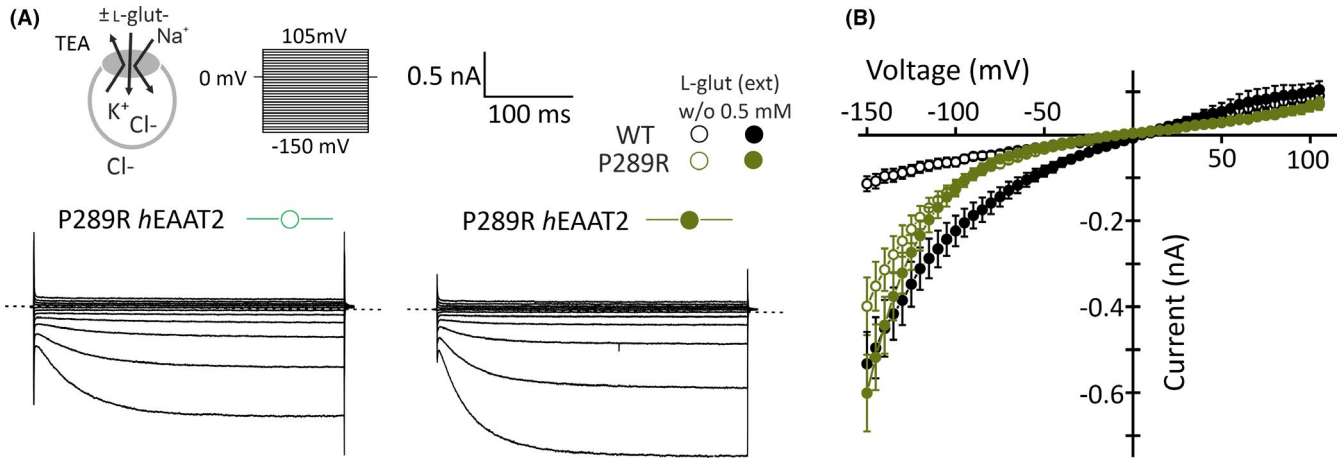

FIGURE 6 Epileptic encephalopathy (EE)–associated mutation P289R changes the amplitude and the time and voltage dependence of human excitatory amino acid transporter (*h*EAAT2) anion currents. (A) Representative P289R *h*EAAT2 whole-cell currents under ionic conditions, which permit all transitions between transporter conformations (in mM: ±0.5 L-glutamate$^-$/140 $Na^+Cl^-_{ext}$ and 115 $K^+Cl^-_{int}$). (B) Mean current-voltage relationships for WT and P289R *h*EAAT2 without or with external L-glutamate (open/closed symbols, n = 12/15, WT/P289R). Data in B are provided as means ±CI. Color code: WT/P289R: black/green

in cells expressing G82R or P289R and much larger than for WT *h*EAAT2 (Figure 2). L85P and G82R permit permeation of L-glutamate and D-gluconate through *h*EAAT2 anion channels. Our functional results are in full agreement with current structural concepts about the EAAT anion channel pore, in which L85 functions as pore-forming residue projecting its side chain into the aqueous permeation pathway formed at the interface between the trimerization and the mobile transport domain.[11,26,27] Substitution of leucine 85 by proline or glycine 82 by arginine might modify the dimensions of the anion channel pore and permit passage of D-gluconate and L-glutamate, which both have diameters too large to permeate through the WT *h*EAAT2 anion channel. The functional consequences of the L85P mutation have been recently addressed in another study that mostly quantified L-glutamate uptake by radiotracer experiments.[45] This study reported decreased L-glutamate uptake in mammalian cells expressing L85P *h*EAAT2 and reduced WT uptake upon co-expression of L85P, suggesting a dominant-negative effect on L-glutamate transport. EAAT2 anion currents were not taken into consideration; however, L85P *h*EAAT2-mediated L-glutamate efflux can fully account for their experimental results.

G82R and L85P are—to our knowledge—the first mutations that modify the size selectivity of EAAT anion channels. Glutamate is a potent neurotoxin, and a key physiological function of the EAATs is to accumulate L-glutamate over large concentration gradients and to ensure low resting L-glutamate concentration in the extracellular space. Such function requires a strict selectivity against L-glutamate of the EAAT anion channels. Under ischemic conditions, activation of volume-activated VRAC anion channels is known to permit L-glutamate efflux, causing excessive L-glutamate release and brain damage.[46–48] Glutamate-permeable mutant EAAT2 anion channels could serve a similar pathological function in EE. EAAT2 is not only present in astrocytes, but also in presynaptic nerve terminals.[7,8] Because neurons lack significant glutamine-synthase activity, intracellular L-glutamate levels are larger in neurons than in astrocytes predicting higher L-glutamate effluxes through presynaptic mutant EAAT2. In both cases, extracellular glutamate homeostasis will be significantly altered, possibly causing neuronal death and brain atrophy via glutamate excitotoxicity.

SLC1A2-associated epileptic syndromes exhibit a clinical phenotype[1,2] that is far more severe than for many other EEs (please see the case reports of Guella et al[1]). All patients experienced epileptic seizures within the first weeks of life and showed significant developmental delay, and all exhibit cerebral, but not cerebellar, atrophy.[1–3] Patients with the G82R mutation presented with prolonged focal motor seizures that started as left clonic leg jerks and later with bilateral tonic-clonic seizures.[1] In case of L85P, continuous multifocal twitching, particularly in sleep, was observed at an age of 2 days. Later, generalized and focal myoclonic seizures occurred.[2] The patient with the P289R mutation had myoclonic jerks and absence and gelastic seizures.[1] As his case was reported, the patient was 6-years-old with 50 seizures daily on a combined treatment of rufinamide, levetiracetam, nitrazepam, and the ketogenic diet.[1] The L85P mutation was associated with the almost complete absence of myelination of cerebrum, but normal myelination of the cerebellum and brainstem at 1 year, and at the age of 13 years, extreme supratectorial atrophy involving the cortex, deep gray matter, and white matter, with normal-sized brainstem and cerebellum.[2] Whereas patients with G82R had progressive generalized atrophy of the cerebrum, MRI of the P289R patients revealed only an asymmetric brainstem of unlikely clinical significance at an age of 3 years. Because all patients with EE-associated *SLC1A2* mutations have therapy-resistant seizures with early onset and high frequency, cerebral atrophy associated with G82R and L85P is likely due to the additional glutamate permeability of these two mutations. The more pronounced cerebral atrophy of patients with the L85P than with the G82R mutations might be explained by differences in intracellular trafficking. L85P only slightly affects ER exit and surface membrane insertion so that heterozygous patients with this variant may exhibit higher numbers of mutant transporters in the surface membrane than patients with the G82R mutation.

P289R does not increase D-gluconate permeability of *h*EAAT2 anion channels. However, it causes pronounced gain-of-function of *h*EAAT2 chloride currents, resulting in large increases of P289R *h*EAAT2 anion currents, despite strongly reduced surface expression of these mutant transporters (Figure 1). The functional consequences of P289R mutation on *h*EAAT2 transport functions are identical to those of the P290R on *h*EAAT1. The *SLC1A3* mutation causes episodic ataxia type 6[13] via gain-of-anion channel function with prominent inward-rectification and decreased L-glutamate uptake.[14] The $Slc1a3^{P290R/+}$ mouse has pronounced epilepsy,[15] whereas $Slc1a3^{-/-}$ mice—that do not express EAAT1/GLAST—exhibit only mild ataxia. The comparison of these two animal models demonstrates that the gain of function of EAAT1 anion channels is sufficient to cause epilepsy. EAAT2 contributes to setting $[Cl^-]_{int}$ in cortical but not in hippocampal astrocytes.[49] Increased activity of mutant EAAT2 anion

channels might decrease astrocytic $[Cl^-]_{int}$ and reduces external [GABA] by enhancing the driving force for GABA transporters (GATs) in this brain region. In *Slc1a3*$^{P290R/+}$ we observed pronounced degenerative effects only in Bergmann glial cells, but not in astrocytes. *SLC1A2*-associated brain atrophy was most pronounced for patients carrying the L85P mutations. Whereas it is tempting to assign the pronounced degeneration to increased L-glutamate permeability of L85P, delayed myelination and nonprogressive cerebral atrophy in patients with P289R may be due to epileptic seizures or to chloride efflux–induced apoptosis as observed in *Slc1a3*$^{P290R/+}$ Bergmann glia.[15]

Monogenetic diseases provide links of altered function of individual proteins to cell and organ dysfunction and insights into molecular mechanisms of protein functions. *SLC1A2* mutations in EE result in exchanges of amino acids that are in proximity to the EAAT2 anion pore.[11] The EAAT anion channel has been studied for decades using a combination of mutagenesis and functional assays, but still no engineered mutations have been described that modify the size selectivity of the pore. Unselective EAAT2 anion channels result in a most severe epileptic phenotype, and pharmaceutical maneuvers that prevent anion channel opening might provide a causative treatment of these disabling syndromes. Because anion channel opening is closely linked to the L-glutamate transport,[11] blocking transporter function will prevent anion channel opening. However, since EAAT2 glutamate transport is necessary for normal brain function,[8,9] this approach does not appear to be helpful. Molecular simulations have described anion channel openings as branching transitions from the transport cycle, that is, that anion channels can open from certain states, but this opening is not required for further progression of the transport cycle.[11] It might be possible to prevent such transitions by pharmacological approaches, and thus obtained compounds might not only be useful in treating *SLC1A2*-associated EEs but also acquired syndromes with increased EAAT anion channel activity.

ACKNOWLEDGMENTS

We would like to thank Dr. M. Hediger, Universität Bern, for providing the expression construct for *h*EAAT2. We also thank Jan Marienhagen from the Institute of Bio- and Geosciences, Biotechnology (IBG-1) of the Forschungszentrum Jülich GmbH for assistance with FACS sorting of KO *LRCC8A* HEK293T cells and Petra Thelen for excellent technical assistance. This work was supported by the German Ministry of Education and Research (E-RARE network Treat-ION, BMBF 01GM1907C to ChF). Open access funding enabled and organized by ProjektDEAL.

CONFLICT OF INTEREST

The authors declare no conflict of interest. We confirm that we have read the Journal's position on issues involved in ethical publication and that our report is consistent with these guidelines.

AUTHOR CONTRIBUTIONS

PK and ChF designed the study and wrote the paper. PK and YK collected and analyzed biochemical and electrophysiological data. PK and ChF designed and created the figures. AF conducted mutagenesis of EAAT2 constructs and performed Crisp-Cas mediated knock-down of *LRCC8A* in HEK293T cells.

ORCID

Peter Kovermann https://orcid.org/0000-0001-5296-4918
Yulia Kolobkova https://orcid.org/0000-0001-9933-2918
Christoph Fahlke https://orcid.org/0000-0001-8602-9952

REFERENCES

1. Guella I, McKenzie MB, Evans DM, Buerki SE, Toyota EB, Van Allen MI, et al. *De Novo* mutations in *YWHAG* cause early-onset epilepsy. Am J Hum Genet. 2017;101(2):300–10.
2. Epi4K, Epilepsy Phenome/Genome Project. *De Novo* mutations in *SLC1A2* and *CACNA1A* are important causes of epileptic encephalopathies. Am J Hum Genet. 2016;99(2):287–98.
3. Epi4K Consortium, Epilepsy Phenome/Genome Project, Allen AS, Berkovic SF, Cossette P, Delanty N, et al. *De novo* mutations in epileptic encephalopathies. Nature. 2013;501(7466):217–21.
4. Pines G, Danbolt NC, Bjoras M, Zhang Y, Bendahan A, Eide L, et al. Cloning and expression of a rat brain L-glutamate transporter. Nature. 1992;360(6403):464–7.
5. Chaudhry FA, Lehre KP, van Lookeren CM, Ottersen OP, Danbolt NC, Storm-Mathisen J. Glutamate transporters in glial plasma membranes: highly differentiated localizations revealed by quantitative ultrastructural immunocytochemistry. Neuron. 1995;15(3):711–20.
6. Schreiner AE, Durry S, Aida T, Stock MC, Rüther U, Tanaka K, et al. Laminar and subcellular heterogeneity of GLAST and GLT-1 immunoreactivity in the developing postnatal mouse hippocampus. J Comp Neurol. 2014;522(1):204–24.
7. Petr GT, Sun Y, Frederick NM, Zhou Y, Dhamne SC, Hameed MQ, et al. Conditional deletion of the glutamate transporter GLT-1 reveals that astrocytic GLT-1 protects against fatal epilepsy while neuronal GLT-1 contributes significantly to glutamate uptake into synaptosomes. J Neurosci. 2015;35(13):5187–201.
8. Rimmele TS, Rosenberg PA. GLT-1: the elusive presynaptic glutamate transporter. Neurochem Int. 2016;98:19–28.
9. Tanaka K, Watase K, Manabe T, Yamada K, Watanabe M, Takahashi K, et al. Epilepsy and exacerbation of brain injury in mice lacking the glutamate transporter GLT-1. Science. 1997;276(5319):1699–702.

10. Wadiche JI, Amara SG, Kavanaugh MP. Ion fluxes associated with excitatory amino acid transport. Neuron. 1995;15(3):721–8.
11. Machtens JP, Kortzak D, Lansche C, Leinenweber A, Kilian P, Begemann B, et al. Mechanisms of anion conduction by coupled glutamate transporters. Cell. 2015;160(3):542–53.
12. Fahlke C, Kortzak D, Machtens JP. Molecular physiology of EAAT anion channels. Pflugers Arch. 2016;468(3):491–502.
13. Jen JC, Wan J, Palos TP, Howard BD, Baloh RW. Mutation in the glutamate transporter EAAT1 causes episodic ataxia, hemiplegia, and seizures. Neurology. 2005;65(4):529–34.
14. Winter N, Kovermann P, Fahlke C. A point mutation associated with episodic ataxia 6 increases glutamate transporter anion currents. Brain. 2012;135(Pt 11):3416–25.
15. Kovermann P, Untiet V, Kolobkova Y, Engels M, Baader S, Schilling K, et al. Increased glutamate transporter-associated anion currents cause glial apoptosis in episodic ataxia 6. Brain Commun. 2020;2(1):fcaa022.
16. Chivukula AS, Suslova M, Kortzak D, Kovermann P, Fahlke C. Functional consequences of *SLC1A3* mutations associated with episodic ataxia 6. Hum Mut. 2020;41(11):1892–905.
17. Garcia-Olivares J, Alekov A, Boroumand MR, Begemann B, Hidalgo P, Fahlke C. Gating of human ClC-2 chloride channels and regulation by carboxy-terminal domains. J Physiol. 2008;586(22):5325–36.
18. Ran FA, Hsu PD, Wright J, Agarwala V, Scott DA, Zhang F. Genome engineering using the CRISPR-Cas9 system. Nat Protoc. 2013;8(11):2281–308.
19. Kovermann P, Machtens JP, Ewers D, Fahlke C. A conserved aspartate determines pore properties of anion channels associated with excitatory amino acid transporter 4 (EAAT4). J Biol Chem. 2010;285(31):23676–86.
20. Melzer N, Torres-Salazar D, Fahlke C. A dynamic switch between inhibitory and excitatory currents in a neuronal glutamate transporter. Proc Natl Acad Sci USA. 2005;102(52):19214–8.
21. Schindelin J, Arganda-Carreras I, Frise E, Kaynig V, Longair M, Pietzsch T, et al. Fiji: an open-source platform for biological-image analysis. Nat Methods. 2012;9(7):676–82.
22. Kovermann P, Hessel M, Kortzak D, Jen JC, Koch J, Fahlke C, et al. Impaired K^+ binding to glial glutamate transporter EAAT1 in migraine. Sci Rep. 2017;7(1):13913.
23. Reyes N, Ginter C, Boudker O. Transport mechanism of a bacterial homologue of glutamate transporters. Nature. 2009;462(7275):880–5.
24. Crisman TJ, Qu S, Kanner BI, Forrest LR. Inward-facing conformation of glutamate transporters as revealed by their inverted-topology structural repeats. Proc Natl Acad Sci USA. 2009;106(49):20752–7.
25. Garaeva AA, Oostergetel GT, Gati C, Guskov A, Paulino C, Slotboom DJ. Cryo-EM structure of the human neutral amino acid transporter ASCT2. Nat Struct Mol Biol. 2018;25(6):515–21.
26. Cheng MH, Torres-Salazar D, Gonzalez-Suarez AD, Amara SG, Bahar I. Substrate transport and anion permeation proceed through distinct pathways in glutamate transporters. eLife. 2017;6:e25850.
27. Chen I, Pant S, Wu Q, Cater RJ, Sobti M, Vandenberg RJ, et al. Glutamate transporters have a chloride channel with two hydrophobic gates. Nature. 2021;591(7849):327–31.
28. Hotzy J, Schneider N, Kovermann P, Fahlke C. Mutating a conserved proline residue within the trimerization domain modifies Na^+ binding to excitatory amino acid transporters and associated conformational changes. J Biol Chem. 2013;288(51):36492–501.
29. Kolen B, Kortzak D, Franzen A, Fahlke C. An amino-terminal point mutation increases EAAT2 anion currents without affecting glutamate transport rates. J Biol Chem. 2020;295(44):14936–47.
30. Gendreau S, Voswinkel S, Torres-Salazar D, Lang N, Heidtmann H, Detro-Dassen S, et al. A trimeric quaternary structure is conserved in bacterial and human glutamate transporters. J Biol Chem. 2004;279(38):39505–12.
31. Mim C, Balani P, Rauen T, Grewer C. The glutamate transporter subtypes EAAT4 and EAATs 1–3 transport glutamate with dramatically different kinetics and voltage dependence but share a common uptake mechanism. J Gen Physiol. 2005;126(6):571–89.
32. Wadiche JI, Kavanaugh MP. Macroscopic and microscopic properties of a cloned glutamate transporter/chloride channel. J Neurosci. 1998;18(19):7650–61.
33. Zerangue N, Kavanaugh MP. Flux coupling in a neuronal glutamate transporter. Nature. 1996;383(6601):634–7.
34. Alleva C, Kovalev K, Astashkin R, Berndt MI, Baeken C, Balandin T, et al. Na^+-dependent gate dynamics and electrostatic attraction ensure substrate coupling in glutamate transporters. Sci Adv. 2020;6(47):eaba9854.
35. Kortzak D, Alleva C, Weyand I, Ewers D, Zimmermann MI, Franzen A, et al. Allosteric gate modulation confers K^+ coupling in glutamate transporters. EMBO J. 2019;38(19):e101468.
36. Watzke N, Bamberg E, Grewer C. Early intermediates in the transport cycle of the neuronal excitatory amino acid carrier EAAC1. J Gen Physiol. 2001;117(6):547–62.
37. Leinenweber A, Machtens JP, Begemann B, Fahlke C. Regulation of glial glutamate transporters by C-terminal domains. J Biol Chem. 2011;286(3):1927–37.
38. Pedersen SF, Okada Y, Nilius B. Biophysics and physiology of the volume-regulated anion channel (VRAC)/volume-sensitive outwardly rectifying anion channel (VSOR). Pflugers Arch. 2016;468(3):371–83.
39. Voss FK, Ullrich F, Munch J, Lazarow K, Lutter D, Mah N, et al. Identification of LRRC8 heteromers as an essential component of the volume-regulated anion channel VRAC. Science. 2014;344(6184):634–8.
40. Schanzler M, Fahlke C. Anion transport by the cochlear motor protein prestin. J Physiol. 2012;590(2):259–72.
41. Ronstedt K, Sternberg D, Detro-Dassen S, Gramkow T, Begemann B, Becher T, et al. Impaired surface membrane insertion of homo- and heterodimeric human muscle chloride channels carrying amino-terminal myotonia-causing mutations. Sci Rep. 2015;5:15382.
42. Kalser J, Cross JH. The epileptic encephalopathy jungle – from Dr West to the concepts of aetiology-related and developmental encephalopathies. Curr Opin Neurol. 2018;31(2):216–22.
43. Scheffer IE, Berkovic S, Capovilla G, Connolly MB, French J, Guilhoto L, et al. ILAE classification of the epilepsies: position paper of the ILAE Commission for Classification and Terminology. Epilepsia. 2017;58(4):512–21.
44. Howell KB, Harvey AS, Archer JS. Epileptic encephalopathy: use and misuse of a clinically and conceptually important concept. Epilepsia. 2016;57(3):343–7.
45. Stergachis AB, Pujol-Giménez J, Gyimesi G, Fuster D, Albano G, Troxler M, et al. Recurrent *SLC1A2* variants cause epilepsy via a dominant negative mechanism. Ann Neurol. 2019;85(6):921–6.

46. Yang J, Vitery MDC, Chen J, Osei-Owusu J, Chu J, Qiu Z. Glutamate-releasing SWELL1 channel in astrocytes modulates synaptic transmission and promotes brain damage in stroke. Neuron. 2019;102(4):813–27.e6.
47. Mongin AA. Volume-regulated anion channel–a frenemy within the brain. Pflugers Arch. 2016;468(3):421–41.
48. Hyzinski-Garcia MC, Rudkouskaya A, Mongin AA. LRRC8A protein is indispensable for swelling-activated and ATP-induced release of excitatory amino acids in rat astrocytes. J Physiol. 2014;592(22):4855–62.
49. Lehre KP, Danbolt NC. The number of glutamate transporter subtype molecules at glutamatergic synapses: chemical and stereological quantification in young adult rat brain. J Neurosci. 1998;18(21):8751–7.

SUPPORTING INFORMATION

Additional supporting information may be found in the online version of the article at the publisher's website.

How to cite this article: Kovermann P, Kolobkova Y, Franzen A, Fahlke C. Mutations associated with epileptic encephalopathy modify EAAT2 anion channel function. Epilepsia. 2021;00:1–14. https://doi.org/10.1111/epi.17154